

**Partial fusion of a cytochrome P450 system by carboxy-terminal  
attachment of putidaredoxin reductase to P450cam (CYP101A1)**

Eachan O. Johnson<sup>#</sup> and Luet-Lok Wong<sup>\*</sup>

Department of Chemistry, University of Oxford, Inorganic Chemistry Laboratory, South  
Parks Road, Oxford OX1 3QR, UK

<sup>#</sup> Current Address: Broad Institute of MIT and Harvard, 415 Main Street, Cambridge, MA  
02142, USA

<sup>\*</sup> Corresponding author

E-mail: [luet.wong@chem.ox.ac.uk](mailto:luet.wong@chem.ox.ac.uk) (LLW)

## Abstract

Cytochrome P450 (CYP) enzymes catalyze the insertion of oxygen into carbon-hydrogen bonds and have great potential for enzymatic synthesis. Application development of class I CYPs is hampered by their dependence on two redox partners (a ferredoxin and ferredoxin reductase), slowing catalysis compared to self-sufficient CYPs such as CYP102A1 (P450BM3). Previous attempts to address this have fused all three components in several permutations and geometries, with much reduced activity compared to the native system. We report here the new approach of fusing putidaredoxin reductase (PdR) to the carboxy-terminus of CYP101A1 (P450cam) via a linker peptide and reconstituting camphor hydroxylase activity with free putidaredoxin (Pdx). Initial purification of a P450cam-PdR fusion yielded 2.0% heme incorporation. Co-expression of *E. coli* ferrochelatase, lengthening the linker from 5 to 20 residues, and altering culture conditions for enzyme production furnished 85% heme content. Fusion co-expression with Pdx gave a functional system with comparable *in vivo* camphor oxidation activity as the native system. *In vitro*, the fused system's steady state NADH oxidation rate was two-fold faster than that of the native system. In contrast to the native system, NADH oxidation rates for the fusion enzyme showed non-hyperbolic dependence on Pdx concentration, suggesting a role for the PdR domain; these data were consistent with a kinetic model based on two-site binding of Pdx by P450cam-PdR and inactive dimer formation of the fusion. P450cam-PdR is the first example of a class I P450 fusion that exhibits significantly more favorable behavior than that of the native system.

## Introduction

The heme-dependent cytochrome P450 (CYP) superfamily of monooxygenases are found in most domains of life,<sup>1</sup> from hepatocytes<sup>2</sup> and mitochondria,<sup>3</sup> through plants,<sup>4</sup> nematodes,<sup>5</sup> and bacteria,<sup>6, 7</sup> to protozoa,<sup>8, 9</sup> and viruses.<sup>10</sup> Their varied provenances mirror their varied functions; even within a particular species, several P450s with differentiated activities and specificities can be found, testament to the biological importance of insertion of an oxygen atom into a carbon-hydrogen bond, the fundamental reaction commonly catalyzed by these enzymes.<sup>11</sup>

CYP systems solve the problem of delivering the two necessary reducing equivalents from NAD(P)H to the cytochrome synchronously with its hydroxylating catalytic cycle in several ways.<sup>11</sup> *Eukaryota* employ several permutations of fused redox domains and *Bacteria* and mitochondria often, but not exclusively, rely on shuttle ferredoxins to provide electrons.<sup>12</sup> Bacterial class I CYP systems are commonly composed of an FAD-dependent ferredoxin reductase, and a [2Fe-2S]-dependent ferredoxin, and the terminal P450 monooxygenase (Fig. 1A).<sup>13</sup> Each of these components is usually highly specific, ensuring tight regulation of electron transport and preventing cross talk between multiple systems in the same cell. The three-component nature of these systems generates inherent kinetic impedance for substrate oxidation when compared to one- (e.g. CYP102A1 (P450BM3) from *Bacillus megaterium*<sup>14</sup>) or two-component CYP systems (e.g. vertebrate hepatic CYP3A4<sup>15</sup>) since electron transfer is intermolecular rather than largely intramolecular. As a shuttle protein, the class I ferredoxins must be able to recognize and bind both the ferredoxin reductase and CYP enzyme to give [2Fe-2S]:heme or [2Fe-2S]:FAD orbital overlap for a physiologically appropriate rate of electron transfer. Under physiological conditions, the first electron transfer to the ferric, substrate-bound CYP from the reduced ferredoxin controls the NAD(P)H-oxidation and substrate hydroxylation rates of class I systems.

The most studied class I cytochrome P450 is the camphor 5-hydroxylase P450cam (CYP101A1) from *Pseudomonas putida*. P450cam and its cognate electron transfer partners—the FAD-dependent putidaredoxin reductase (PdR) and the [2Fe-2S] putidaredoxin (Pdx)—have been structurally characterized.<sup>16-20</sup> As a result of the extensive body of biochemical and structural data, the P450cam system is considered the model of the bacterial class I CYPs, despite its idiosyncrasies.<sup>21</sup> This class contains a multitude of other CYPs with potential for biotechnological applications but their kinetic properties inhibit widespread development.<sup>22</sup> Numerous CYPs are not genetically associated with their physiological electron transfer partners, including those from metagenomic libraries. Activity reconstitution

relies on the opportune activity of known CYP-associated ferredoxins such as Pdx,<sup>23, 24</sup> and adrenodoxin (Adx) associated with the mitochondrial CYP11A1 (P450<sub>scc</sub>),<sup>25-30</sup> amongst others.<sup>31-36</sup> If these problems were resolved, processes could be facilitated in fields as diverse as fine chemicals and pharmaceuticals,<sup>37</sup> e.g. *in vitro* synthesis of antibiotics by uncultivable soil bacteria might become viable.<sup>38, 39</sup>

Previous approaches have mimicked the naturally fused CYPs.<sup>40, 41</sup> Every permutation of a chain of P450cam, Pdx and PdR was constructed and expressed (Fig. 1B); all such fusions showed slower *in vivo* camphor biotransformation than the native system.<sup>42</sup> The P450cam system components have been attached to a synthetic non-natural ternary linker;<sup>43</sup> in other work, they were fused to the subunits of proliferating cell nuclear antigen (PCNA), a hetero-trimer from *Sulfolobus solfataricus*, to form a self-assembling, branched super-enzyme (Fig. 1C).<sup>44, 45, 46</sup> These approaches illustrated the importance of flexibility in such class I fusion systems to allow potentially orthogonal binding orientations between redox partners for efficient electron shuttling by the ferredoxin. Class I CYPs have also been fused to the carboxy-terminus of the reductase domain of P450Rh<sub>f</sub> from *Rhodococcus rhodochrous* (Fig. 1D), but electron transfer rates were low.<sup>47, 48</sup>

Since fusion of complete systems had seen limited success, we explored the creation of fusions using only a subset of the P450cam system components, namely PdR and P450cam (Fig. 1E), and investigated the electron transfer and camphor oxidation kinetics of the system *in vivo* and *in vitro*. Partial fusion of CYP system enzymes has been reported: PdR was chemically cross-linked to Pdx, which improved camphor hydroxylation kinetics at saturating P450cam concentrations.<sup>49</sup> However, fusing of indirect redox partners has not been described. After constructing a series of expression plasmids and optimizing conditions for production of a maximally heme-incorporated P450cam-PdR fusion enzyme, we found that this fused system oxidized DL-camphor identically to the native system *in vivo*. We demonstrated enhanced electron transfer, and found that NADH oxidation *in vitro* showed non-Michaelis-Menten dependence on Pdx concentration, which could be modeled by considering an extended two-site sequential binding model that incorporates two distinct Pdx binding sites and inactive dimerization of the fully Pdx-bound P450cam-PdR fusion.

## Materials and methods

### *Molecular biology*

Genes encoding P450cam and PdR had previously been cloned into expression plasmids.<sup>50</sup> The *camC* gene was amplified with primers incorporating NcoI and SacI restriction sites and a sequence encoding a carboxy-terminal AAKKT linker (linker A, LA), while primers incorporating SacI and HindIII sites were used to amplify *camA*. Amplified fragments were assembled in the Multiple Cloning Site 1 (MCS1) of an NcoI/HindIII-linearized pRSFDuet-1 vector in a three-piece ligation step. This pRSFDuet::*camC-LA-camA* construct is referred to as pFusion.

*E. coli* ferrochelatase, encoded by *hemH*, was amplified from genomic DNA, which had been isolated using the Promega Genomic DNA Miniprep kit according to the manufacturer's instructions. PCR primers incorporating NdeI and XhoI restriction sites allowed ligation into the MCS2 of NdeI/XhoI-linearized pFusion to create the recombinant plasmid pRSFDuet::*camC-LA-camA::hemH*, or pFusionH.

The original AAKKT linker in pFusionH was replaced with the sequence DVSTEQSAKEAPAETLGAFR (linker 2, L2) by the MEGAprimer WHOLE Plasmid (MEGAWHOP) method.<sup>51, 52</sup> pFusionH was linearized by inverse PCR, which excluded the linker region. Exactly complementary oligonucleotides containing the sequence encoding L2 and a *ca.* 10-nt 5'- and 3'-overlap with the linearized plasmid was synthesized (Eurofins MWG Biotech, Germany) and used as a primer pair to amplify the linearized plasmid (Table S1). After DpnI digest, the PCR product (a doubly-nicked plasmid) was then used to transform *E. coli* DH5 $\alpha$ , from which the intact plasmid pRSFDuet::*camC-L2-camA* (pFusionH2), was extracted and the insert sequences confirmed by Sanger sequencing (Source Bioscience, UK).

### *Expression and purification of P450cam, Pdx, and PdR*

The *camC* gene encoding the non-dimerizing P450cam mutant C334A was used throughout, and is referred to as the native enzyme.<sup>53</sup> Expression plasmids harboring the *camA*, *camB* and *camC* genes, encoding the PdR, Pdx, and native P450cam enzymes, respectively, had previously been constructed in our laboratory. The expression and purification of these proteins have already been described.<sup>54, 55</sup>

### *Expression and purification of fused P450cam-PdR enzymes*

A colony of *E. coli* BL21 (DE3) transformed with the appropriate pFusion plasmid and grown on LB agar containing 30  $\mu\text{g mL}^{-1}$  kanamycin (kan) was used to inoculate a starter culture of TB containing 30  $\mu\text{g mL}^{-1}$  kan (TB<sub>kan</sub>). This culture was grown until OD<sub>600</sub> was

0.5–0.8 and used to inoculate a large-scale TB<sub>kan</sub> culture at 2% v/v. The large culture was grown at 37 °C and 200 rpm until OD<sub>600</sub> was 0.6–0.8. The temperature was then reduced to 20 °C, and shaking was reduced to 100 rpm. The culture was supplemented with 1 mM 5-aminolevulinic acid ( $\delta$ -ALA), 0.1 mM riboflavin, 4 mM ammonium ferric citrate (AFC), and 1 mM DL-camphor from a 100 mM stock in ethanol. After two hours, enzyme production was induced with 40  $\mu$ M isopropyl  $\beta$ -D-1-thiogalactopyranoside (IPTG).

Expression was continued for 72 h, or until the culture reached saturation (OD<sub>600</sub>  $\approx$  8), at which point the cells were harvested by centrifugation at 4000  $\times$  g and 4 °C, before being stored at –20 °C. To extract the fusion enzyme, cells were thawed at 4 °C and then resuspended in 10 mM Tris-HCl, pH 7.4, supplemented with 20% v/v glycerol, 1% v/v Triton X-100, 1 mM DTT, 0.5% v/v  $\beta$ -mercaptoethanol (BME), 1 mM camphor, and 0.1 mg mL<sup>–1</sup> lysozyme from chicken egg white (Sigma-Aldrich, UK), ensuring cell wet weight was  $\leq$  20% w/v of the final suspension. This suspension was incubated at 4 °C for 2 h before cells were lysed by sonication. Cell debris were removed by centrifugation at 39,000  $\times$  g and 4 °C.

The cell-free lysate was loaded onto a 200  $\times$  50 mm DEAE-Sepharose (GE Healthcare, UK) column and eluted with a gradient of 60–200 mM KCl (P450cam-LA-PdR), or 80–230 mM KCl (P450cam-L2-PdR) in 50 mM Tris-HCl pH 7.4, supplemented with 1 mM camphor. Red-colored fractions were then concentrated by ultrafiltration and desalted on a 500 mL bed-volume Sephadex G-25 (GE Healthcare, UK) column, which had been equilibrated in 50 mM Tris-HCl, pH 7.4.

Eluate from the G-25 column was concentrated by ultrafiltration and applied to a 120  $\times$  26 mm Source 15Q column (GE Healthcare, UK), and eluted with a gradient of 50–700 mM KCl (P450cam-LA-PdR) or 100–750 mM KCl (P450cam-L2-PdR) in 50 mM Tris-HCl, pH 7.4. The purest fractions, as indicated by  $A_{420}/A_{280} \geq 1$ , were pooled, concentrated to ca. 100  $\mu$ M, and filtered through a 0.22  $\mu$ m sterile syringe filter. Sterile glycerol was added to 50% v/v for storage at –20 °C. Glycerol was removed immediately prior to experiments by gel filtration on a PD-10 column (GE Healthcare, UK) equilibrated with 40 mM phosphate buffer, pH 7.4. The P450 content was determined by the CO-difference spectrum method and using  $\epsilon_{450-490} = 91 \text{ mM}^{-1}\text{cm}^{-1}$ .<sup>56, 57</sup>

### ***Camphor-binding titrations***

All titrations were performed at 30  $\pm$  0.5 °C. P450cam or P450cam-L2-PdR was diluted to 2–5  $\mu$ M using 40 mM phosphate, pH 7.4, in 2.5 ml, and 0.5–2  $\mu$ L of DL-camphor was added using a Hamilton syringe from a 1, 10, or 100 mM stock solution in ethanol. After mixing,

the peak-to-trough absorbance difference,  $\Delta A$ , was recorded on a Cary 50 spectrophotometer between 700 nm and 250 nm. Further aliquots of camphor were added until  $\Delta A$  did not change further. The observed  $\Delta A$  values were scaled for dilution, and the dissociation constant,  $K_d$ , for camphor binding was obtained by fitting the scaled  $\Delta A$  to the camphor concentration using a rectangular hyperbola:  $\Delta A = \Delta A_{\max} \times [\text{camphor}]/(K_d + [\text{camphor}])$ . The titrations were repeated with 200 mM KCl added from a 2 M stock solution in 40 mM phosphate, pH 7.4 before the addition of camphor aliquots.

#### **Potassium-binding titrations**

Potassium binding titrations were carried out in 50 mM Tris-HCl buffer, pH 7.4, in 2.5 ml. The P450cam-L2-PdR fusion was buffer exchanged to the Tris-HCl buffer by elution through a PD-10 column. DL-Camphor was added as a 100 mM stock solution in ethanol to a final concentration of 1 mM. Aliquots of a 2 M stock of KCl in 50 mM Tris-HCl, pH 7.4, were added and the difference spectrum recorded until a final KCl concentration of 200 mM. The peak-to-trough difference  $\Delta A$  was scaled to account for dilution and the dissociation constant,  $K_d$ , for potassium binding was determined by fitting the scaled  $\Delta A$  values to KCl concentration using a rectangular hyperbola:  $\Delta A = \Delta A_{\max} \times [\text{KCl}]/(K_d + [\text{KCl}])$ .

#### **Camphor biotransformation**

*E. coli* BL21 (DE3) cells were co-transformed with an appropriate pFusion plasmid and pCW::camB, and an isolated colony from the LB<sub>amp/kan</sub> agar plate was used to inoculate LB<sub>amp/kan</sub> medium. The culture was shaken overnight at 37 °C and 200 rpm, and then used to inoculate a large-scale TB<sub>amp/kan</sub> culture at 10% v/v. After 5 h at 37 °C and 200 rpm, 1 mM 5-aminolevulinic acid ( $\delta$ -ALA), 0.1 mM riboflavin, 4 mM and ammonium ferric citrate (AFC) were added and the temperature was lowered to 30 °C. After one hour, 40  $\mu$ M IPTG was added to induce expression of the camphor-oxidation system at 30 °C and 200 rpm for 16 h.

After centrifugation at  $4000 \times g$  and 4 °C for 10 min, cell pellets were resuspended in 20% of their original culture volume in TB<sub>amp/kan</sub> containing 1% w/v glucose. The P450 content was *ca.* 20 nM in both the fusion and native whole cell reactions after 24 h. The culture was transferred to 2 L baffled flasks, with 200 mL culture per flask. DL-camphor was added to 4 mM from a 100 mM stock in ethanol. Aliquots of 900  $\mu$ L samples of culture were taken at several time points up to 24 h. 9-Hydroxyfluorene (75  $\mu$ M) was added as an internal standard and the sample was extracted with 400  $\mu$ L ethyl acetate.<sup>50</sup> After phase separation by centrifugation at  $13,400 \times g$  for 1 min the organic phase was analyzed on a ThermoFinnigan Trace GC instrument equipped with a flame ionization detector, an AutoSampler AS3000 and

a 30 m DB-1 fused silica column (0.32 mm diameter, 0.25  $\mu$ m film thickness). The oven temperature was held at 80  $^{\circ}$ C for 1 min then increased to 220  $^{\circ}$ C over 9 min, and held at 220  $^{\circ}$ C for 2 min. Helium was used as the carrier gas. The 24 h extracts were also analyzed by GC-MS to confirm product identities.

Serially diluting an aqueous indole (Sigma-Aldrich, UK) solution in volumetric flasks generated a series of indole standards spanning 75  $\mu$ M to 2.4 mM. Ethyl acetate extracts of these standards were prepared as above; the resultant GC chromatograms were used to calculate a standard curve of the detector response normalized to internal standard against indole concentration.

### ***NADH turnover assays***

All turnover assays were carried out using a Cary 50 spectrophotometer at  $30.0 \pm 0.5$   $^{\circ}$ C in a 1.2 mL solution of 40 mM phosphate buffer, pH 7.4. Bovine liver catalase (100  $\mu$ g mL $^{-1}$ ) was added to all reactions containing DL-camphor. Mixtures were allowed to equilibrate for 2 min before reaction initiation.

Steady state NADH oxidation assays were performed in triplicate using 0.5  $\mu$ M PdR, 5  $\mu$ M Pdx, and 0.5  $\mu$ M P450cam, or 5  $\mu$ M Pdx and 0.5  $\mu$ M P450cam-L2-PdR fusion. NADH was added to *ca.* 320  $\mu$ M to give  $A_{340} = 2$ . The reaction was initiated by adding 1 mM DL-camphor from a 100 mM ethanol stock, and  $A_{340}$  was monitored. NADH oxidation rate was calculated using  $\epsilon_{340} = 6.22$  mM $^{-1}$  cm $^{-1}$ . The reaction mixtures were extracted and analyzed as those from reactions *in vivo*. The ratio of the 5-*exo*-hydroxycamphor product peak area to that of the internal standard was compared to that for the native system to determine the coupling efficiency for camphor oxidation by the fusion enzyme.

Pdx titrations for NADH oxidation were performed in triplicate using 0.1  $\mu$ M P450cam with 0.5  $\mu$ M PdR, or 0.1, 0.5, or 1.0  $\mu$ M P450cam-L2-PdR fusion with and without 0.4  $\mu$ M PdR. NADH was added as above. The reaction was initiated by adding 1 mM DL-camphor from a 100 mM ethanol stock, and  $A_{340}$  was monitored. NADH oxidation rate was calculated as above. Titrations against native P450cam produced a good non-linear least squares fit to the Michaelis-Menten model; those against the fusion displayed non-Michaelis-Menten behavior, and were initially analyzed by ordinary least squares fitting of the Hanes-Woolf rearrangement of the Michaelis-Menten model:  $[Pdx]/v = [Pdx]/k_{cat}[Fus] + K_m/k_{cat}[Fus]$ .

Ferricyanide was used as the terminal electron acceptor to measure NADH oxidation by PdR or the PdR domain of the fused P450cam-L2-PdR enzyme. The reaction mixture

contained 10 nM PdR or P450cam-PdR. NADH was added as above. The reaction was initiated by adding 1 mM  $K_3Fe(CN)_6$ .  $A_{420}$  was monitored over time, and  $K_3Fe(CN)_6$  reduction rates were calculated using  $\epsilon_{420} = 1.04 \text{ mM}^{-1} \text{ cm}^{-1}$ .

### *Spectral decomposition*

Samples of pure P450cam and PdR were used to generate UV-visible spectra standards, which were used as a basis set for spectral decomposition of the UV-visible spectrum of the P450cam-PdR fusions, allowing calculation of heme incorporation. Briefly, the spectrum of the fusion protein was treated as a vector of absorbance values, for which the contribution from P450cam and PdR was calculated by solving the system of linear equations in Eq. 1 to find  $\mathbf{c}$ , where  $\mathbf{a}$  is a vector of length  $m$  corresponding to the absorbance measurements of the fusion at  $m$  wavelengths,  $\mathbf{E}$  is a  $2 \times m$  matrix containing the absorbances of the standards, and  $\mathbf{c}$  is a vector of length 2 containing the relative contribution from each standard.

$$\mathbf{a} = \mathbf{E}\mathbf{c} \quad \text{Eq. 1}$$

Since  $\mathbf{E}$  is not a square matrix, this system cannot be solved using  $\mathbf{c} = \mathbf{E}^{-1}\mathbf{a}$ . However, the relation in Eq. 2 may be used. If the  $\mathbf{e}_{1j}$  are the P450cam absorbances and the  $\mathbf{e}_{2j}$  are the PdR absorbances, then heme incorporation was calculated by  $100 \times c_1/c_2$ .

$$\mathbf{c} = (\mathbf{E}^T\mathbf{E})^{-1}\mathbf{E}^T\mathbf{a} \quad \text{Eq. 2}$$

## Results and discussion

### *Production and purification of fused P450cam-PdR*

Previous reports of CYP fusions suggested pivotal and unpredictable effects of both the length and nature of the linker.<sup>42, 43</sup> The plasmid pRSFDuet-1, with two multiple cloning sites (MCS) each downstream of a T7-promoter, was used for heterologous expression in *E. coli*. The genes encoding PdR and P450cam-C334A were assembled with a five amino-acid linker (LA, sequence AAKKT, Fig. 2A & 2B, Table S1) in MCS1 of pRSFDuet-1 to produce the construct pRSFDuet::*camC-LA-camA* (pFusion, Fig. 2C). Previous studies had shown the benefit of expressing hemoproteins in the presence of ferrochelatase (HemH).<sup>58</sup> The *E. coli* *hemH* gene was amplified and cloned into MCS2 of pFusion to give the pFusionH construct pRSFDuet::*camC-LA-camA::hemH*.

The linker AAKKT was chosen because previous work on the crystal structure of fused CYP11A1 and Adx showed that it produced a good compromise between stability and activity.<sup>59</sup> However, since the fusions in the present study were instead between CYP (P450cam) and reductase (PdR) domains, a second linker was designed to mimic that found in P450BM3, a natural fusion of a diflavin reductase domain and a CYP domain.<sup>14</sup> This linker (L2) had the sequence DVSTEQSAKEAPAETLGAFR and led to the construct pRSFDuet::*camC-L2-camA::hemH* (pFusionH2, Fig. 2C).

After inducing P450cam-LA-PdR expression from pFusion, enzyme purification followed the typical protocol for P450cam isolation.<sup>54</sup> Spectral decomposition of the UV-visible spectrum of the product against P450cam and PdR standards indicated that the fusion enzyme was severely heme-depleted, showing heme incorporation of 2.0% (Fig. 3A). To improve heme incorporation, supplementation of the culture medium was explored (Table 1). Initial supplementation with 100  $\mu$ M  $\delta$ -ALA, the committed heme precursor, and iron in the form of 10  $\mu$ M FeCl<sub>2</sub>, gave a modest increase in heme content to 5.8% (Fig. 3B). Increasing the  $\delta$ -ALA concentration to 500  $\mu$ M raised the heme content to 26% while FeCl<sub>2</sub> at 50  $\mu$ M had a similar effect (6.9% heme content) as combining 100  $\mu$ M  $\delta$ -ALA with 10  $\mu$ M FeCl<sub>2</sub>. Addition of 1 mM DL-camphor on its own, without other supplements, resulted in much higher heme incorporation (31%). On the other hand the presence of 2 mM Na<sub>2</sub>EDTA reduced heme assimilation to 8.6%. These observations indicated that higher heme flux from supplementing with  $\delta$ -ALA and FeCl<sub>2</sub> and stabilization of the P450cam fold by camphor binding increased holoenzyme production, while binding of iron by EDTA<sup>4-</sup> lowered the heme flux and hence reduced the production of active enzyme. The pFusionH construct,

which co-expressed ferrochelatase, furnished a heme content of 22% in the presence of 100  $\mu$ M  $\delta$ -ALA, a significant improvement over the 5.8% heme content using pFusion.

Similar trends in heme content with culture conditions were observed with the fusion containing the longer L2 linker (data not shown). A set of conditions for higher heme incorporation into P450cam-PdR fusions was established as follows: the concentration of iron in the culture medium during fusion expression was raised to 4 mM by using the non-toxic soluble iron source ammonium ferric citrate (AFC), with 1 mM DL-camphor to stabilize the P450cam structure, 1 mM of the heme precursor  $\delta$ -ALA, 100  $\mu$ M riboflavin to promote FAD synthesis, and co-expression of HemH. Under these conditions the pFusionH2 construct yielded the P450cam-L2-PdR fusion enzyme with 85% heme incorporation (Table 1, Fig. 3D). This enzyme was used for biochemical investigations.

#### ***In vivo activity of the P450cam-L2-PdR fusion***

The activity of the fused (P450cam-L2-PdR, Pdx) and native (P450cam, Pdx, PdR) systems for whole-cell biotransformation of DL-camphor was compared over 24 h. *E. coli* BL21 (DE3) was transformed either with pFusionH2 and pCW::*camB*, or pRSFDuet::*camC*::*camA* and pCW::*camB* plasmids and used for *in vivo* camphor oxidation. SDS-PAGE analysis showed that pFusionH2-transformed cultures expressed a polypeptide at the expected size of P450cam-L2-PdR, and that all enzymes necessary to reconstitute camphor 5-hydroxylase activity were expressed (Fig. S1). Adjusted to the same P450 content, cultures expressing the fusion enzyme oxidized DL-camphor at a similar rate to the native system (Fig. 4), with both showing >99% camphor conversion after 1 hour. Interestingly, further oxidation of 5-*exo*-hydroxycamphor to 5-oxo-camphor by the fusion enzyme was 39% lower than for the native system.

GC-MS analysis identified indole in the culture supernatants (Fig. 4A & S2), with 4-fold higher concentration in the reaction with the fusion compared to the native system. When the cell growth and biotransformation were carried out in FB<sub>glycerol</sub>, a minimal medium, no indole was detected in either reaction (Fig. S3). It was not clear what caused these differences.

#### ***In vitro activity of the P450cam-PdR fusion***

The CO-difference spectrum of purified P450cam-L2-PdR fusion enzyme showed the 450 nm Sorét band characteristic of the CYP superfamily (Fig. 5A) with a minor shoulder at 420 nm indicative of a small amount of misfolded hemoprotein.<sup>56, 60</sup>

The electron transfer property of the PdR domain in the fusion was assessed by the rate of ferricyanide reduction. For free PdR the rate of electron transfer from the reduced FAD to the small molecule acceptor  $\text{Fe}(\text{CN})_6^{3-}$  is sufficiently fast to provide an indirect measure of the rate of FAD reduction by NADH.<sup>12, 61, 62</sup> The rate constants of FAD reduction of native PdR ( $1500 \pm 200 \text{ s}^{-1}$ ) and P450cam-L2-PdR ( $1550 \pm 20 \text{ s}^{-1}$ ) were identical within experimental error.

Substrate binding by native ferric P450cam is accompanied by conversion of the heme from a low- to a high-spin state, as shown by the shift of the Sorét maximum from 419 nm to 390 nm. The fused system also exhibited this characteristic behavior (Fig. 5B & S4). P450cam is also unusual in displaying cooperative camphor binding with potassium binding.<sup>54, 63</sup> The binding of potassium stabilizes an otherwise unfavorable conformation around Tyr96 that orientates its phenol side chain into the substrate pocket where it forms a hydrogen bond with the camphor carbonyl oxygen and tightens camphor binding. The  $K_d$  for camphor binding by the P450cam-L2-PdR fusion in 40 mM phosphate buffer was  $7 \pm 1 \text{ }\mu\text{M}$  (Fig. 5C), decreasing to  $2.0 \pm 0.1 \text{ }\mu\text{M}$  in the presence of 200 mM KCl. The  $K_d$  value for native P450cam with 200 mM KCl was  $1.2 \pm 0.1 \text{ }\mu\text{M}$ . The  $K_d$  for potassium binding by the fusion was  $11.9 \pm 0.2 \text{ mM}$  (Fig. 5D), compared to  $5.4 \pm 0.5 \text{ mM}$  for native P450cam.<sup>54</sup> These data showed that the potassium binding site was intact in the fusion enzyme and there was cooperative binding of potassium and camphor. However, the fusion of PdR appeared to weaken both camphor and potassium binding, possibly also due to occlusion of the active site or the potassium binding site by the PdR-domain.<sup>54, 64</sup>

Next, the *in vitro* NADH oxidation activity of the reconstituted P450cam-L2-PdR fusion with camphor as substrate was assayed and compared to the native system. When 5  $\mu\text{M}$  Pdx is mixed with 0.5  $\mu\text{M}$  P450cam-L2-PdR, or with 0.5  $\mu\text{M}$  P450cam and 0.5  $\mu\text{M}$  PdR, the 10:1:1 Pdx:P450cam:PdR ratio results in the first electron transfer from reduced Pdx to ferric P450cam being rate-determining. The NADH oxidation rates were  $7.8 \pm 0.3 \text{ nmol (nmol P450cam)}^{-1} \text{ s}^{-1}$  and  $17 \pm 0.1 \text{ nmol (nmol P450cam-L2-PdR)}^{-1} \text{ s}^{-1}$ . Hence, the fusion accepted electrons from reduced Pdx more than twice as quickly than in the native system under these conditions. Such an improvement has not been reported for a fused P450cam enzyme or any other fused class I CYP system. Previous fusions linked the entire

three-component system into a single polypeptide (Fig. 1B) but recent structural studies of the Pdx:P450cam complex showed that orientation of the components is a crucial aspect of efficient electron transfer.<sup>19, 65</sup> The C-terminal Trp106 of Pdx is known from structural and biochemical studies to be critical for the P450cam:Pdx interaction.<sup>66</sup> A C-terminal truncated Adx is more efficient at transferring electrons to and hence reconstitute the activity of non-native CYPs.<sup>25, 67, 68</sup> Fusions must be flexible enough to enable the enzymes to adopt optimal positions relative to each other. It can be envisioned that there might not be sufficient flexibility in triple fusions for this to occur. With a P450cam-PdR fusion, Pdx would not be constrained by fusion to another protein. Moreover, the proximity of PdR (from which Pdx receives an electron) to P450cam (to which Pdx donates an electron) could lead to higher turnover rates, i.e. a proximity effect. GC analysis of the products of camphor oxidation catalyzed by the fusion enzyme *in vitro* (Fig. S5) showed >90 % coupling of NADH-derived electrons to 5-*exo*-hydroxycamphor formation, a comparable value to that of the native system.<sup>54</sup>

Initial rates of NADH oxidation for the fused and native CYP enzymes were measured in the presence of 1 mM DL-camphor and varying concentrations of Pdx to assess the P450cam:Pdx interaction and electron transfer. For assays with native P450cam, an equal concentration of PdR was also present. Under these conditions the first electron transfer from Pdx<sup>r</sup> to ferric P450cam is the slowest step,<sup>12</sup> and native P450cam showed single-site Michaelis-Menten behavior with a  $k_{\text{cat}}$  of  $64 \pm 3 \text{ s}^{-1}$  (Fig. 6A).<sup>69</sup> On the other hand, the Hanes-Woolf plot of initial NADH oxidation rate by 0.1  $\mu\text{M}$  P450cam-L2-PdR against Pdx concentration showed significant deviation from linearity, in particular at low Pdx concentrations where a distinct up-tick in  $[\text{Pdx}]/v$  was observed (Fig. 6B). The apparent  $k_{\text{cat}}$  was estimated to be  $56 \text{ s}^{-1}$  from a single-site fit. The kinetics with fusion concentrations of 0.5 and 1.0  $\mu\text{M}$  showed more pronounced deviation from Michaelis-Menten kinetics, as well as decreased apparent  $k_{\text{cat}}$  with increasing enzyme concentration (estimated  $k_{\text{cat}} = 46 \text{ s}^{-1}$  at 0.5  $\mu\text{M}$  and  $38 \text{ s}^{-1}$  at 1.0  $\mu\text{M}$ , Fig. 6B).

Since measurement of the Fdx<sup>r</sup>-to-CYP electron transfer rate is usually carried out in the presence of sufficient FdR to ensure that this step is rate determining,<sup>70</sup> initial NADH oxidation rates were measured for 0.1  $\mu\text{M}$  P450cam-L2-PdR, varying concentrations of Pdx, and 0.4  $\mu\text{M}$  PdR. Under these conditions, the Hanes-Woolf plots were also non-linear, but with a distinct down-tick in  $[\text{Pdx}]/v$  at low Pdx concentrations (Fig. 6C).

## Development of a kinetic model for fused P450cam-L2-PdR

Increasing the fusion enzyme concentration increased the apparent cooperativity of the enzyme-Pdx interaction while reducing the apparent  $k_{cat}$ , an unusual phenomenon. Since the two Pdx-binding sites of the P450cam-PdR fusion were not equivalent, usual models (like the Hill equation) of cooperative multi-site binding were, perhaps not surprisingly, inappropriate. Instead, a derivative of the sequential-binding kinetic model was considered.<sup>71, 72</sup> In this model, substrate (Pdx in the present case) molecules may bind an enzyme in either a particular sequence or randomly,<sup>73</sup> but only one or more of the complexes produce the measured activity with independent rate constants  $k_{cat,i}$ . Instantaneous equilibrium is a simplifying assumption of this model. The observation that the native P450cam system displayed Michaelis-Menten kinetics and that a mixture of 0.1  $\mu$ M P450cam-PdR and 0.4  $\mu$ M PdR showed Michaelis-Menten kinetics at lower Pdx concentrations but more fusion-like behavior at high Pdx concentrations led us to propose a model for the kinetics of the fusion enzyme. The model (Fig. 7A) is based on several assumptions: (a) PdR reduction to PdR<sup>r</sup> by NADH is orders of magnitude faster than reduction of ferric camphor-bound P450cam by Pdx<sup>r</sup>, (b) reduction of oxidized Pdx (Pdx<sup>o</sup>) to Pdx<sup>r</sup> by PdR<sup>r</sup> is fast under these conditions,<sup>12</sup> (c) all P450cam domains are substrate-bound in the presence of 1 mM DL-camphor, and (d) P450cam:Pdx<sup>r</sup> binding occurs in preference to PdR:Pdx<sup>r</sup> binding, since dissociation of newly-reduced Pdx<sup>r</sup> from PdR avoids product inhibition and allows the Pdx<sup>r</sup> to interact with P450cam as soon as possible.<sup>74, 75</sup>

In this model the fused, camphor-bound ferric P450cam domain forms a complex with Pdx<sup>r</sup> with a dissociation constant  $K_{d1}$ . This complex can undergo electron transfer ( $k_{cat1}$ ) or the PdR domain can bind and reduce a Pdx<sup>o</sup> molecule as a Pdx<sup>r</sup> equivalent ( $K_{d2}$ ), since Pdx<sup>o</sup> reduction is fast. The Pdx<sup>r</sup>:Fus:Pdx<sup>r</sup> complex can then either revert to Fus:Pdx<sup>r</sup>, or reduce the camphor-bound ferric P450cam domain ( $k_{cat2}$ ). When free PdR is added to the solution, this ternary complex becomes rare because free reductase competes for binding and reduction of Pdx<sup>o</sup> ( $K_{d4}$ ,  $k_{cat3}$ ). Finally, the lowering of  $k_{cat}$  with increasing fusion enzyme concentration suggested the formation of an inactive dimeric form. This possibility is taken into account by an equilibrium between the ternary Pdx<sup>r</sup>:Fus:Pdx<sup>r</sup> complex with another fusion enzyme molecule to form a catalytically inactive quaternary complex ( $K_{d3}$ ), although other dimerization mechanisms may exist. Based on this model, the initial rate of NADH oxidation is given by Eq. 3:

$$-\frac{d[\text{NADH}]}{dt} = [\text{Fus}] \frac{k_{\text{cat}1} \frac{[\text{Pdx}]}{K_{\text{d}1}} + k_{\text{cat}2} \frac{[\text{Pdx}]^2}{K_{\text{d}1}K_{\text{d}2}} + k_{\text{cat}3} \frac{[\text{Pdx}]^2[\text{PdR}]}{K_{\text{d}1}K_{\text{d}2}K_{\text{d}4}}}{1 + \frac{[\text{Pdx}]}{K_{\text{d}1}} + \frac{[\text{Pdx}]^2}{K_{\text{d}1}K_{\text{d}2}} + \frac{[\text{Pdx}]^2[\text{Fus}]}{K_{\text{d}1}K_{\text{d}2}K_{\text{d}3}} + \frac{[\text{Pdx}]^2[\text{PdR}]}{K_{\text{d}1}K_{\text{d}2}K_{\text{d}4}}} \quad \text{Eq. 3}$$

where the  $K_{\text{d},i}$  are the dissociation constants and the  $k_{\text{cat},j}$  are the rate constants for electron transfer for the complexes in Fig. 7A.

In order to avoid over-fitting and over-parameterization, initial fitting to Eq. 3 varied only terms containing  $K_{\text{d}1}$ ,  $K_{\text{d}2}$ ,  $K_{\text{d}3}$ ,  $k_{\text{cat}1}$ , and  $k_{\text{cat}2}$  using the data collected in the absence of free PdR (Fig. 8A). The remaining parameters  $K_{\text{d}4}$  and  $k_{\text{cat}3}$  were then fit to all the data while holding the other parameters fixed (Fig. 8B). This approach produced a reasonable fit for most of the data although there were some residual deviations at low Pdx concentration.

The fitted values show that binding of the first Pdx molecule by the fusion enzyme is weaker than for the native system ( $K_{\text{d}1} = 17 \pm 2 \mu\text{M}$  compared to  $K_{\text{m}} = 7.0 \pm 0.8 \mu\text{M}$ ), possibly because the PdR domain occludes the Pdx binding site in the fusion. In light of weaker camphor and potassium binding observed for the P450cam domain of the fusion compared to the native enzyme, weaker  $\text{Pdx}^{\text{r}}$  binding is not surprising. The fitted value for  $k_{\text{cat}1}$  was  $53 \pm 7 \text{ s}^{-1}$ , close to the value of  $64 \pm 3 \text{ s}^{-1}$  for  $k_{\text{cat}}$ , the corresponding parameter for the Michaelis-Menten model of  $\text{Pdx}^{\text{r}}$  binding and oxidation by native P450cam.

The dissociation constant of the second Pdx binding event ( $K_{\text{d}2} = 8 \pm 2 \mu\text{M}$ ) is smaller than the first, and identical within experimental error to the native system's  $K_{\text{m}}$  (Fig. 8A). Multi-site enzymes often display cooperativity, a phenomenon where successive binding events become increasingly thermodynamically favorable, due to conformational changes in the protein.<sup>76</sup> Since the P450cam-PdR fusion is an artificial enzyme, it might not be expected that such an effect would be observed. However, the second  $\text{Pdx}^{\text{r}}$  binding event may occur through several mechanisms, including nascent  $\text{Pdx}^{\text{r}}$  moving from the fused PdR domain, or by  $\text{Pdx}^{\text{r}}$  from bulk solution interacting with the P450cam domain. Therefore, the decrease in  $K_{\text{d}2}$  compared to  $K_{\text{d}1}$  could be attributed to a proximity effect arising from fusion of the Pdx-reducing PdR domain to P450cam.

$\text{Pdx}^{\text{r}}$  oxidation by the ternary complex ( $k_{\text{cat}2} = 42 \pm 2 \text{ s}^{-1}$ ) is marginally slower than by the binary complex ( $k_{\text{cat}1} = 53 \pm 7 \text{ s}^{-1}$ ). It is possible that the contribution to  $K_{\text{d}2}$  from rapid  $\text{Pdx}^{\text{o}}$  recruitment and reduction to  $\text{Pdx}^{\text{r}}$ —which then could switch to the adjacent P450cam domain—by the PdR domain, while it manifests as tighter binding ( $K_{\text{d}2}$ ), is a multi-step

process which is slower than simple  $\text{Pdx}^{\text{r}}$  oxidation by the P450cam domain, represented by  $k_{\text{cat1}}$ .

The catalytically inactive complex of two fusion enzyme molecules and two  $\text{Pdx}$  molecules could explain, in terms of self-inhibition, the empirical decrease in apparent  $k'_{\text{cat}}$  as fused P450cam-PdR enzyme concentration increased (Fig. 6B), in contrast to native P450cam under similar conditions (Fig. 6A). The observed data provide no insight into the structure of the  $[\text{Fus:Pdx}^{\text{r}}]_2$  dimer (Fig. 7A), although it may be envisioned as a homo-dimer of  $\text{Fus:Pdx}^{\text{r}}$  hetero-dimers. The relatively small dissociation constant for this complex ( $K_{\text{d3}} = 1.8 \pm 0.2 \mu\text{M}$ ) may reflect an increase in the interfacial binding area in comparison to a single  $\text{Fus:Pdx}^{\text{r}}$  interaction.

The proposed model also suggests how the addition of free PdR dampens the sigmoidal NADH oxidation kinetics of the fused system by competing with the PdR domain in the fusion enzyme for  $\text{Pdx}$  molecules. The affinity of PdR for  $\text{Pdx}$  ( $K_{\text{d4}} = 0.03 \pm 0.01 \mu\text{M}$ , Fig. 8B) is shown to be two orders of magnitude higher than that of P450cam ( $7.0 \pm 0.8 \mu\text{M}$ , Fig. 6A); such an extreme difference has been seen previously by calorimetry.<sup>77</sup> This proposed model therefore explains the non-linearity of the PdR-supplemented fusion system's hybrid NADH oxidation kinetics (Fig. 6C): at low  $\text{Pdx}$  concentrations, the proximity effect of the fused PdR domain is removed because  $\text{Pdx}^{\text{o}}$  binds preferentially to the free, excess PdR. At higher  $\text{Pdx}$  concentrations,  $\text{Pdx}^{\text{o}}$  binding with the fused PdR is more likely, especially as the native PdR becomes saturated, so the proximity effect (with its attendant potential for inactive dimer formation) is more prevalent.

## Conclusion

Protein recognition and electron transfer between enzymes in class I CYP systems is still not fully understood.<sup>32</sup> Slow kinetics have constrained development of these technologically promising enzymes for applications.<sup>78</sup> We have shown that partial fusion of a class I CYP system can lend it favorable properties. Changes in the linker peptide and addition of common culture supplements enabled the production of the almost fully heme-incorporated CYP-FdR fusion. This system is catalytically active *in vivo* and *in vitro*. In addition to the convenience of such a fusion, the unusual kinetic properties allowed the construction of a reasonable model of binding events. This model may allow future improvements to the fused enzyme, and also facilitate better understanding of ferredoxin-to-CYP electron transfer. As such, partially fused class I CYP systems merit further investigation. Finally, given that PdR can show high activity for the reduction of non-native electron transfer ferredoxins from

other CYP systems, such as Arx from *Novosphingobium aromaticivorans* and Pux from *Rhodopseudomonas palustris*,<sup>79, 80</sup> fusions of CYP enzymes with PdR could be tested for activity reconstitution with native forms as well as engineered variants of these ferredoxins.

#### **Acknowledgments**

The authors are grateful to Sophia Cheng, who carried out some heme incorporation optimization experiments and camphor and potassium chloride titration assays, and Dr Colin Sparrow, who carried out GC-MS data collection and NIST mass spectrum fingerprint analysis.

## 499    **References**

- 500    1.     D. R. Nelson, *Hum. Genomics*, 2009, **4**, 59-65.
- 501    2.     P. A. Williams, J. Cosme, D. M. Vinkovic, A. Ward, H. C. Angove, P. J. Day, C.
- 502         Vonrhein, I. J. Tickle and H. Jhoti, *Science*, 2004, **305**, 683-686.
- 503    3.     A. J. Annalora, D. B. Goodin, W.-X. Hong, Q. Zhang, E. F. Johnson and C. D. Stout,
- 504         *J. Mol. Biol.*, 2010, **396**, 441-451.
- 505    4.     B. Hamberger and S. Bak, *Philos. Trans. R. Soc., B*, 2013, **368**, 20120426-20120426.
- 506    5.     R. Laing, D. J. Bartley, A. A. Morrison, A. Rezansoff, A. Martinelli, S. T. Laing and
- 507         J. S. Gilleard, *Int. J. Parasitol.*, 2015, **45**, 243-251.
- 508    6.     D. Zhu, M.-J. Seo, H. Ikeda and D. E. Cane, *J. Am. Chem. Soc.*, 2011, **133**, 2128-
- 509         2131.
- 510    7.     H. Ouellet, J. B. Johnston and P. R. O. de Montellano, *Arch. Biochem. Biophys.*,
- 511         2010, **493**, 82-95.
- 512    8.     W. Xu, F. F. Hsu, E. Baykal, J. Huang and K. Zhang, *PLoS Pathog.*, 2014, **10**,
- 513         e1004427.
- 514    9.     C. K. Chen, P. S. Doyle, L. V. Yermalitskaya, Z. B. Mackey, K. K. H. Ang, J. H.
- 515         McKerrow and L. M. Podust, *PLoS Negl. Trop. Dis.*, 2009, **3**, 3-12.
- 516    10.    D. C. Lamb, L. Lei, A. G. Warrilow, G. I. Lepesheva, J. G. Mullins, M. R. Waterman
- 517         and S. L. Kelly, *J. Virol.*, 2009, **83**, 8266-8269.
- 518    11.    P. R. O. de Montellano, *Cytochrome P450: Structure, Mechanism, and Biochemistry*,
- 519         Springer, New York, NY, 3rd edn., 2005.
- 520    12.    M. M. Purdy, L. S. Koo, P. R. O. de Montellano and J. P. Klinman, *Biochemistry*,
- 521         2004, **43**, 271-281.
- 522    13.    F. Hannemann, A. Bichet, K. M. Ewen and R. Bernhardt, *Biochim. Biophys. Acta*,
- 523         2007, **1770**, 330-344.
- 524    14.    C. J. C. Whitehouse, S. G. Bell and L.-L. Wong, *Chem. Soc. Rev.*, 2012, **41**, 1218-
- 525         1260.
- 526    15.    Y. Farooq and G. C. Roberts, *Biochem. J.*, 2010, **432**, 485-493.
- 527    16.    T. L. Poulos, B. C. Finzel and A. J. Howard, *J. Mol. Biol.*, 1987, **195**, 687-700.
- 528    17.    I. F. Sevrionkova, T. L. Poulos and I. Y. Churbanova, *J. Biol. Chem.*, 2010, **285**,
- 529         13616-13620.
- 530    18.    T. C. Pochapsky, N. U. Jain, M. Kuti, T. A. Lyons and J. Heymont, *Biochemistry*,
- 531         1999, **38**, 4681-4690.
- 532    19.    S. Tripathi, H. Li and T. L. Poulos, *Science*, 2013, **340**, 1227-1230.
- 533    20.    I. F. Sevrionkova, H. Li and T. L. Poulos, *J. Mol. Biol.*, 2004, **336**, 889-902.
- 534    21.    M. J. Honeychurch, A. O. Hill and L.-L. Wong, *FEBS Lett.*, 1999, **451**, 351-353.
- 535    22.    R. Bernhardt and V. B. Urlacher, *Appl. Microbiol. Biotechnol.*, 2014, **98**, 6185-6203.
- 536    23.    J. A. Peterson and D. M. Mock, *Acta Biol. Med. Ger.*, 1979, **38**, 153-162.
- 537    24.    I. C. Gunsalus and G. C. Wagner, *Methods Enzymol.*, 1978, **52**, 166-188.
- 538    25.    A. Müller, J. J. Müller, Y. a. Muller, H. Uhlmann, R. Bernhardt and U. Heinemann,
- 539         *Structure*, 1998, **6**, 269-280.
- 540    26.    J. D. Lambeth and H. Kamin, *J. Biol. Chem.*, 1979, **254**, 2766-2774.
- 541    27.    D. W. Seybert, J. D. Lambeth and H. Kamin, *J. Biol. Chem.*, 1978, **253**, 8355-8358.
- 542    28.    T. A. Pechurskaya, I. N. Harnastai, I. P. Grabovec, A. A. Gilep and S. A. Usanov,
- 543         *Biochem. Biophys. Res. Commun.*, 2007, **353**, 598-604.
- 544    29.    M. Ringle, Y. Khatri, J. Zapp, F. Hannemann and R. Bernhardt, *Appl. Microbiol.*
- 545         *Biotechnol.*, 2013, **97**, 7741-7754.
- 546    30.    K. M. Ewen, M. Ringle and R. Bernhardt, *IUBMB Life*, 2012, **64**, 506-512.
- 547    31.    S. G. Bell, A. B. H. Tan, E. O. D. Johnson and L.-L. Wong, *Mol. BioSyst.*, 2010, **6**,
- 548         206-214.

- 549 32. S. G. Bell, F. Xu, E. O. D. Johnson, I. M. Forward, M. Bartlam, Z. Rao and L.-L.  
550 Wong, *J. Biol. Inorg. Chem.*, 2010, **15**, 315-328.
- 551 33. S. G. Bell, A. Dale, N. H. Rees and L.-L. Wong, *Appl. Microbiol. Biotechnol.*, 2010,  
552 **86**, 163-175.
- 553 34. W. Yang, S. G. Bell, H. Wang, W. Zhou, N. Hoskins, A. Dale, M. Bartlam, L.-l.  
554 Wong and Z. Rao, *J. Biol. Chem.*, 2010, **285**, 27372-27384.
- 555 35. B. Schiffler, M. Bureik, W. Reinle, E.-C. Müller, F. Hannemann and R. Bernhardt, *J.*  
556 *Inorg. Biochem.*, 2004, **98**, 1229-1237.
- 557 36. K. M. Ewen, F. Hannemann, S. Iametti, A. Morleo and R. Bernhardt, *J. Mol. Biol.*,  
558 2011, **413**, 940-951.
- 559 37. Y. Yoshida, *Biol. Pharm. Bull.*, 2012, **35**, 811-811.
- 560 38. J. R. Cupp-Vickery and T. L. Poulos, *Nat. Struct. Mol. Biol.*, 1995, **2**, 144-153.
- 561 39. L. L. Ling, T. Schneider, A. J. Peoples, A. L. Spoering, I. Engels, B. P. Conlon, A.  
562 Mueller, T. F. Schaberle, D. E. Hughes, S. Epstein, M. Jones, L. Lazarides, V. A.  
563 Steadman, D. R. Cohen, C. R. Felix, K. A. Fetterman, W. P. Millett, A. G. Nitti, A.  
564 M. Zullo, C. Chen and K. Lewis, *Nature*, 2015, **517**, 455-459.
- 565 40. S. J. Sadeghi and G. Gilardi, *Biotechnol. Appl. Biochem.*, 2013, **60**, 102-110.
- 566 41. P. Hlavica, *Biotechnol. Adv.*, 2009, **27**, 103-121.
- 567 42. O. Sibbesen, J. J. de Voss and P. R. O. de Montellano, *J. Biol. Chem.*, 1996, **271**,  
568 22462-22469.
- 569 43. H. Hirakawa, N. Kamiya, T. Tanaka and T. Nagamune, *Protein Eng. Des. Sel.*, 2007,  
570 **20**, 453-459.
- 571 44. H. Hirakawa and T. Nagamune, *ChemBioChem*, 2010, **11**, 1517-1520.
- 572 45. H. Hirakawa, A. Kakitani and T. Nagamune, *Biotechnol. Bioeng.*, 2013, **110**, 1858-  
573 1864.
- 574 46. Tomoaki Haga, Hidehiko Hirakawa and T. Nagamune, *PLoS One*, 2013, **8**.
- 575 47. A. Robin, G. A. Roberts, J. Kisch, F. Sabbadin, G. Grogan, N. Bruce, N. J. Turner and  
576 S. L. Flitsch, *Chem. Commun.*, 2009, 2478-2480.
- 577 48. F. Sabbadin, R. Hyde, A. Robin, E.-M. Hilgarth, M. Delenne, S. Flitsch, N. Turner,  
578 G. Grogan and N. C. Bruce, *ChemBioChem*, 2010, **11**, 987-994.
- 579 49. I. Y. Churbanova, T. L. Poulos and I. F. Sevrioukova, *Biochemistry*, 2010, **49**, 58-67.
- 580 50. R. J. Sowden, S. Yasmin, N. H. Rees, S. G. Bell and L.-L. Wong, *Org. Biomol.*  
581 *Chem.*, 2005, **3**, 57-64.
- 582 51. K. Miyazaki, *Methods Mol. Biol.*, 2003, **231**, 23-28.
- 583 52. K. Miyazaki, in *Methods Enzymol.*, Elsevier Inc., 1 edn., 2011, vol. 498, pp. 399-406.
- 584 53. D. P. Nickerson and L.-L. Wong, *Protein Eng.*, 1997, **10**, 1357-1361.
- 585 54. A. C. G. Westlake, C. F. Harford-Cross, J. Donovan and L.-L. Wong, *Eur. J.*  
586 *Biochem.*, 1999, **265**, 929-935.
- 587 55. J. A. Peterson, M. C. Lorence and B. Amarneh, *J. Biol. Chem.*, 1990, **265**, 6066-6073.
- 588 56. T. Omura and R. Sato, *J. Biol. Chem.*, 1964, **239**, 2370-2378.
- 589 57. T. Omura and R. Sato, *J. Biol. Chem.*, 1962, **237**, 1375-1376.
- 590 58. J. Sudhamsu, M. Kabir, M. V. Airola, B. A. Patel, S.-R. Yeh, D. L. Rousseau and B.  
591 R. Crane, *Protein Expr. Purif.*, 2010, **73**, 78-82.
- 592 59. N. Strushkevich, F. MacKenzie, T. Cherkesova, I. Grabovec, S. Usanov and H.-W.  
593 Park, *Proc. Natl. Acad. Sci. U. S. A.*, 2011, **108**, 10139-10143.
- 594 60. S. A. Martinis, S. R. Blanke, L. P. Hager, S. G. Sligar, G. H. Hoa, J. J. Rux and J. H.  
595 Dawson, *Biochemistry*, 1996, **35**, 14530-14536.
- 596 61. M. Holden, M. Mayhew, D. Bunk, A. Roitberg and V. Vilker, *J. Biol. Chem.*, 1997,  
597 **272**, 21720-21725.

- 598 62. F. Xu, S. G. Bell, Y. Peng, E. O. D. Johnson, M. Bartlam, Z. Rao and L.-L. Wong,  
599 *Proteins*, 2009, **77**, 867-880.
- 600 63. E. Deprez, E. Gill, V. Helms, R. C. Wade and G. Hui Bon Hoa, *J. Inorg. Biochem.*,  
601 2002, **91**, 597-606.
- 602 64. E. Deprez, N. C. Gerber, C. Di Primo, P. Douzou, S. G. Sligar and G. Hui Bon Hoa,  
603 *Biochemistry*, 1994, **33**, 14464- 14468.
- 604 65. Y. Hiruma, M. A. S. Hass, Y. Kikui, W.-M. Liu, B. Ölmez, S. P. Skinner, A. Blok, A.  
605 Kloosterman, H. Koteishi, F. Löhr, H. Schwalbe, M. Nojiri and M. Ubbink, *J. Mol.*  
606 *Biol.*, 2013, **425**, 4353-4365.
- 607 66. W. Zhang, S. S. Pochapsky, T. C. Pochapsky and N. U. Jain, *J. Mol. Biol.*, 2008, **384**,  
608 349-363.
- 609 67. M. Faro, B. Schiffler, A. Heinz, I. Nogués, M. Medina, R. Bernhardt and C. Gómez-  
610 Moreno, *Eur. J. Biochem.*, 2003, **270**, 726-735.
- 611 68. P.-R. Cao and R. Bernhardt, *Eur. J. Biochem.*, 2013, **265**, 152-159.
- 612 69. V. Y. Kuznetsov, T. L. Poulos and I. F. Sevrioukova, *Biochemistry*, 2006, **45**, 11934-  
613 11944.
- 614 70. S. G. Bell, J. H. C. McMillan, J. A. Yorke, E. O. D. Johnson, E. Kavanagh and L.-L.  
615 Wong, *Chem. Commun.*, 2012, **48**, 11692-11694.
- 616 71. L. Pauling, *Proc. Natl. Acad. Sci. U. S. A.*, 1935, **21**, 186-191.
- 617 72. G. S. Adair, *J. Biol. Chem.*, 1925, **63**, 529.
- 618 73. W. W. Chen, M. Niepel and P. K. Sorger, *Genes Dev.*, 2010, **24**, 1861-1875.
- 619 74. V. Y. Kuznetsov, E. Blair, P. J. Farmer, T. L. Poulos, A. Pifferitti and I. F.  
620 Sevrioukova, *J. Biol. Chem.*, 2005, **280**, 16135-16142.
- 621 75. I. F. Sevrioukova, *J. Mol. Biol.*, 2005, **347**, 607-621.
- 622 76. J. Monod, J. Wyman and J.-P. Changeux, *J. Mol. Biol.*, 1965, **12**, 88-118.
- 623 77. M. Aoki, K. Ishimori, H. Fukada, K. Takahashi and I. Morishima, *Biochim. Biophys.*  
624 *Acta*, 1998, **1384**, 180-188.
- 625 78. V. B. Urlacher, S. Lutz-Wahl and R. D. Schmid, *Appl. Microbiol. Biotechnol.*, 2004,  
626 **64**, 317-325.
- 627 79. S. G. Bell and L.-L. Wong, *Biochem. Biophys. Res. Commun.*, 2007, **360**, 666-672.
- 628 80. S. G. Bell, N. Hoskins, F. Xu, D. Caprotti, Z. Rao and L.-L. Wong, *Biochem.*  
629 *Biophys. Res. Commun.*, 2006, **342**, 191-196.

**Table 1.** Summary of heterologous expression conditions for P450cam-PdR fusion constructs and the resultant heme incorporation of the isolated enzyme as calculated by spectral decomposition of its electronic spectrum (see Materials & Methods).  $\delta$ -ALA: 5-aminolevulinic acid, AFC: ammonium ferric citrate, RF: riboflavin, Camphor: DL-camphor, HemH: co-expression of *E. coli* ferrochelatase.

$\delta$ -ALA ( $\mu$ M)	FeCl <sub>2</sub> ( $\mu$ M)	AFC (mM)	RF ( $\mu$ M)	EDTA (mM)	Camphor (mM)	HemH	Linker	Heme (%)
–	–	–	–	–	–	–	LA	2.0
100	10	–	–	–	–	–	LA	5.8
500	–	–	–	–	–	–	LA	26
–	50	–	–	–	–	–	LA	6.9
500	50	–	–	–	–	–	LA	40
–	–	–	–	–	1	–	LA	31
–	–	–	–	2	1	–	LA	8.6
100	–	–	–	–	–	Yes	LA	22
1000	–	4	100	–	1	Yes	L2	85

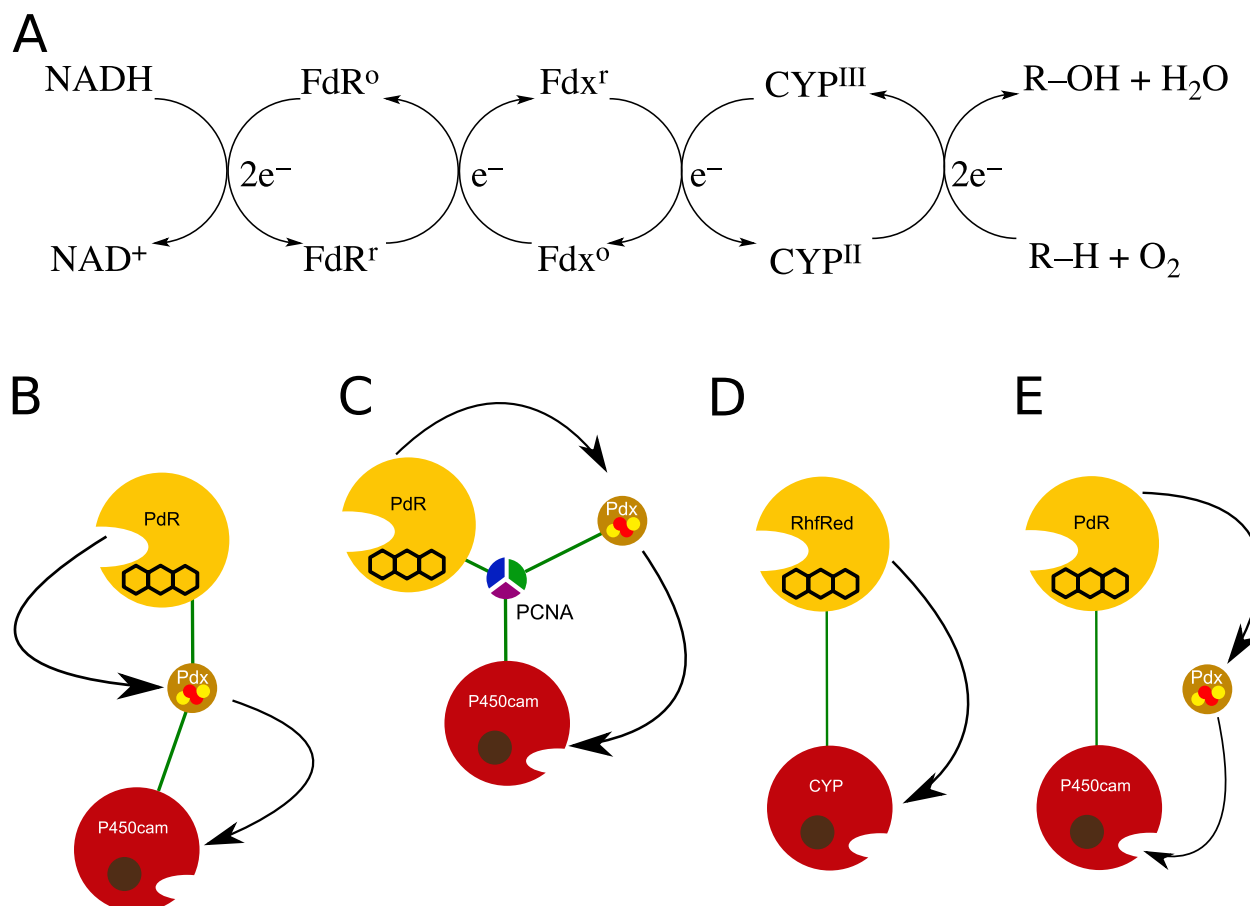


**Fig. 1. Electron-transfer in wild type and artificially fused class I CYP systems.** (A) After NADH oxidation by the ferredoxin reductase (FdR) electrons are shuttled singly by a ferredoxin (Fdx) to the cytochrome P450 (CYP) to catalyze oxygen insertion into a C–H bond. Since this is a relatively slow, intermolecular process, attempts have been made to fuse the three component proteins into a single polypeptide to improve kinetics.<sup>11</sup> (B) Linear fusion of the P450cam system from *Pseudomonas putida* caused a reduction in camphor hydroxylation rate *in vivo*.<sup>42</sup> (C) Fusion of the P450cam system to PCNA, a self-assembling hetero-trimer.<sup>44</sup> (D) The reductase of the P450Rh system from *Rhodococcus rhodocrous* has been systematically fused to a panel of class I P450s, reconstituting the activity of some of them.<sup>47</sup> (E) The present work describes a partially fused P450cam system, with the amino-terminus of PdR connected to the carboxy-terminus of P450cam by a peptide linker, leaving Pdx free to shuttle electrons between the two domains.

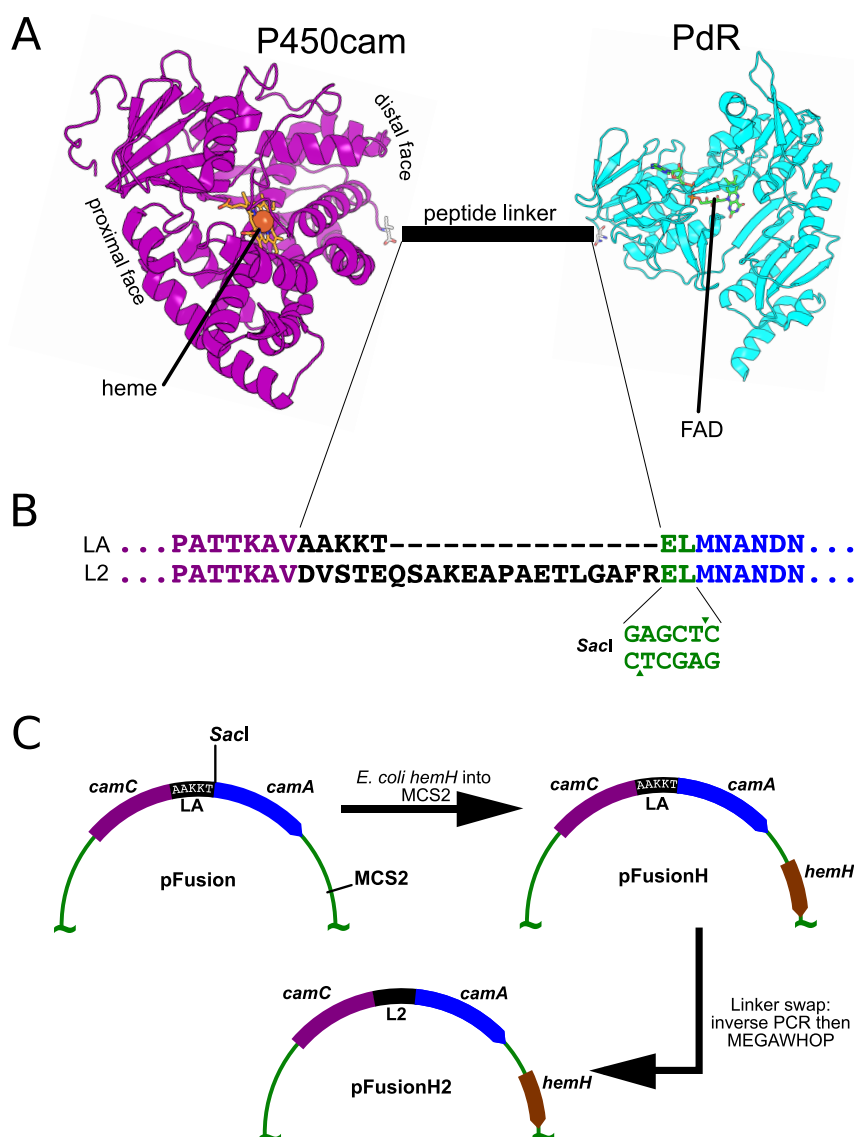


**Fig. 2. Design and construction of fused P450cam-PdR constructs.** The plasmids for P450cam-PdR expression went through three generations of construction. (A) The P450cam and PdR domains were to be linked by a peptide chain connecting the P450cam carboxy-terminus to the PdR amino-terminus. The linker would be encoded in an artificial fused gene. (B) Two linkers were used. The first (LA) was based on work that fused P450scc (CYP11A1) and Adx for crystallization of the enzyme complex, where the AAKKT linker produced a functional fusion protein.<sup>59</sup> The second (L2) contained 20 amino acid residues and was based on the linker found in naturally fused P450BM3 (CYP102A1) from *Bacillus megaterium*. Both linkers were extended due to the incorporation of a *SacI* restriction site. (C) The plasmid pFusion, derived from pRSFDuet-1, was converted to pFusionH by insertion of the *E. coli* ferrochelatase gene (*hemH*) into the second multiple cloning site (MCS2). The third generation plasmid, pFusionH2, was constructed by swapping linker LA for linker L2 using inverse PCR and MEGAWHOP.

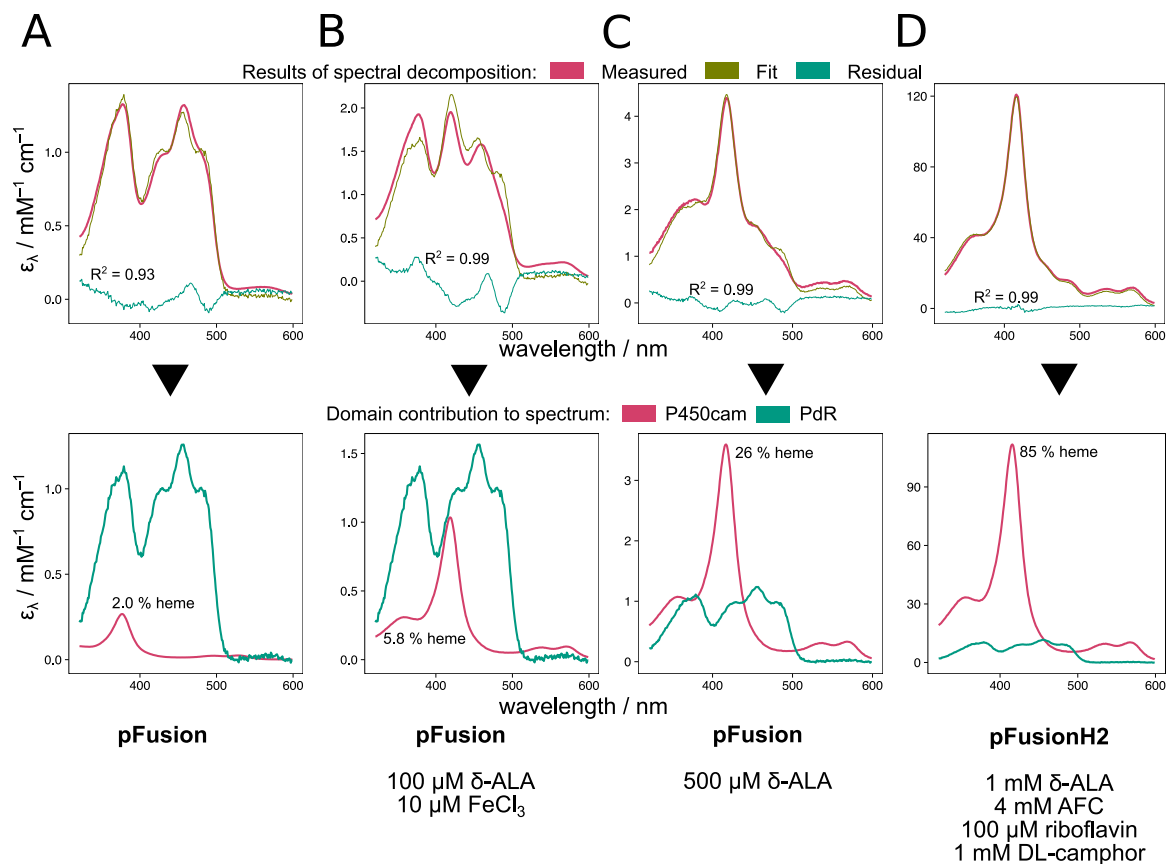


**Fig. 3. Optimization of heme incorporation in fused P450cam-PdR.** Heterologous expression conditions and inter-domain linker length were varied to increase heme incorporation of the P450cam-PdR fusion. (A-D) Heme incorporation for fusion enzymes prepared under several conditions was calculated by spectral decomposition of the electronic spectrum of the purified fusion enzyme based on the spectra of purified native P450cam and PdR. AFC: ammonium ferric citrate.

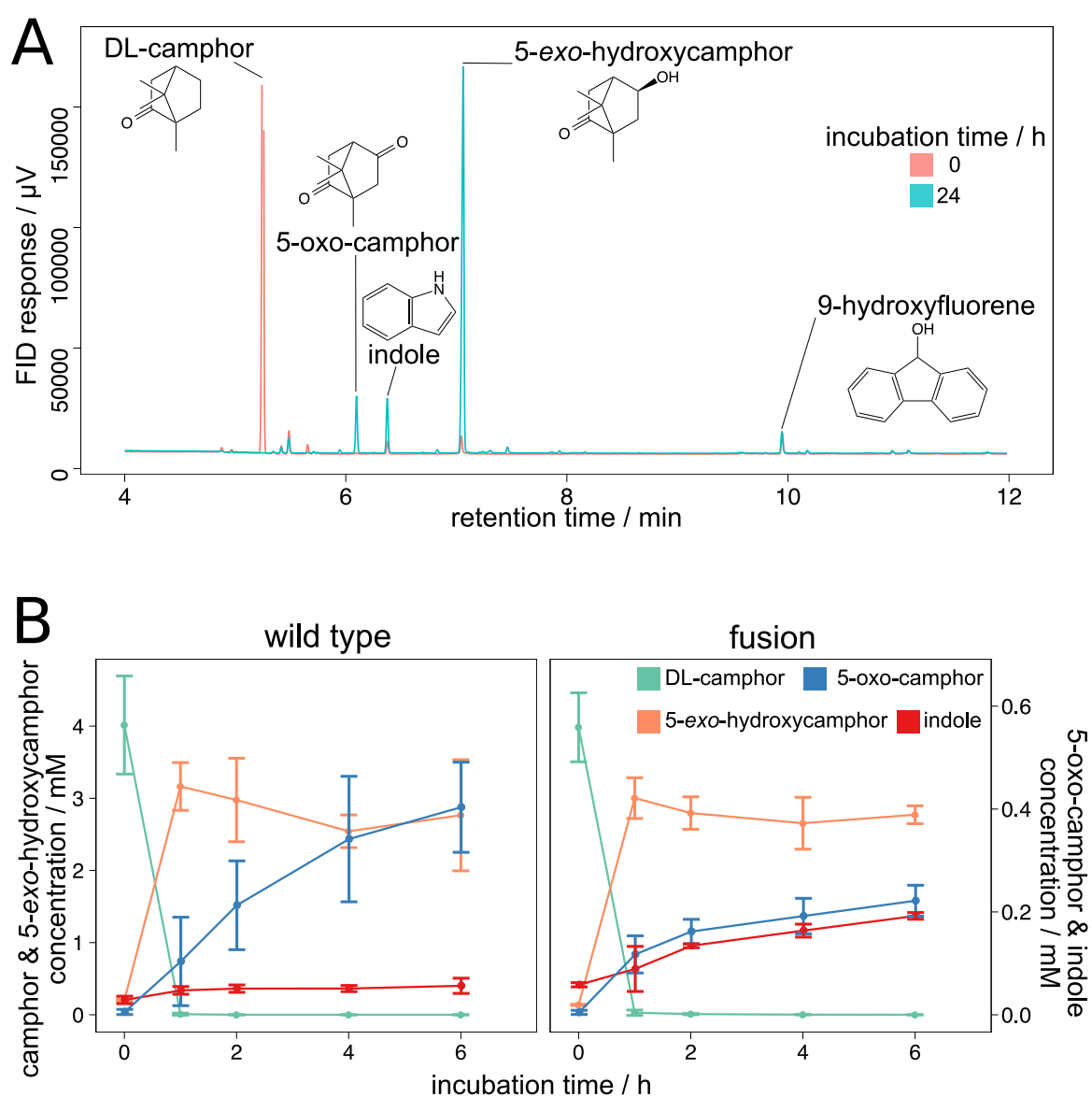


**Fig. 4. *In vivo* activity of the fused P450cam-PdR system in TB medium.** To test the camphor 5-hydroxylase activity of the fused P450cam-PdR system in the presence of Pdx, *E. coli* BL21 (DE3) were transformed with pFusionH2 or pRSFDuet::camA::camC and pUC18::camB and induced in TB, a rich medium, in the presence of 40  $\mu\text{M}$  IPTG and 1 mM DL-camphor. GC analysis was performed on ethyl acetate extracts of culture supernatant (three biological replicates) at several time points until 24 h. (A) Typical GC analysis for culture supernatant from the fused system after 0 and 24 h incubation. (B) The abundance of DL-camphor, 5-*exo*-hydroxycamphor, 5-oxo-camphor, and indole were followed over time. FID = Flame ionization detector.

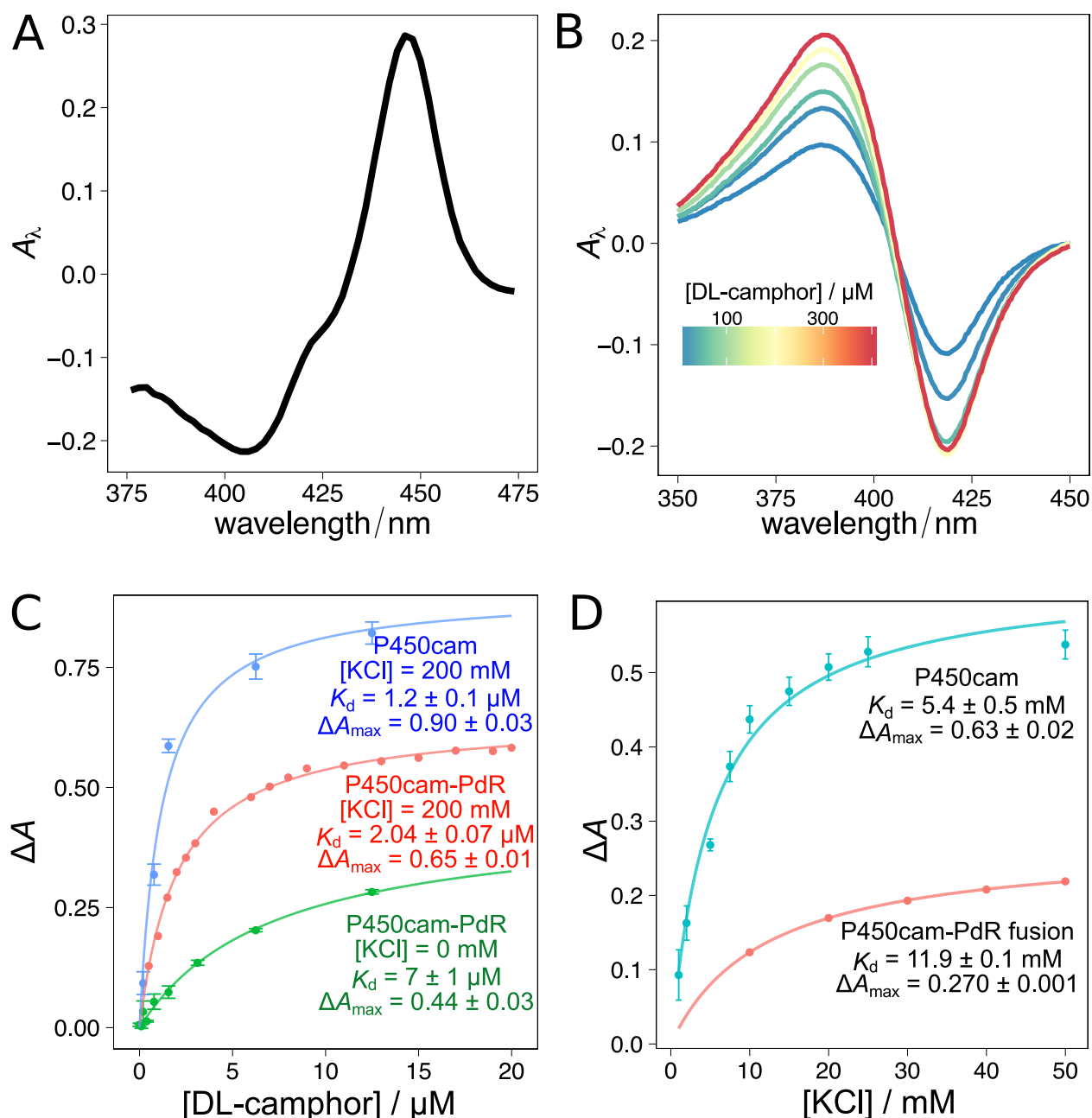


**Fig. 5. Substrate binding of the fused P450cam-PdR enzyme.** (A) Reduced, CO-bound P450cam-PdR fusion has a prominent 450 nm Sorét band, characteristic of the CYP superfamily; the shoulder at 420 nm can be seen, indicative of the inactive P420 form. (B) The Sorét band of ferric P450cam-L2-PdR at 419 nm shifted increasingly to 390 nm with DL-camphor concentration. (C) The maximal Sorét band shift for fused P450cam-PdR was lower than for native P450cam, and the calculated  $K_d$  was two-fold higher in high potassium solution. Lowering the potassium concentration reduced the camphor  $K_d$  for the fusion, mimicking the behavior seen previously in P450cam. (D) Fused P450cam-PdR also had a two-fold higher dissociation constant,  $K_d$ , for potassium ion binding in the presence of excess DL-camphor.

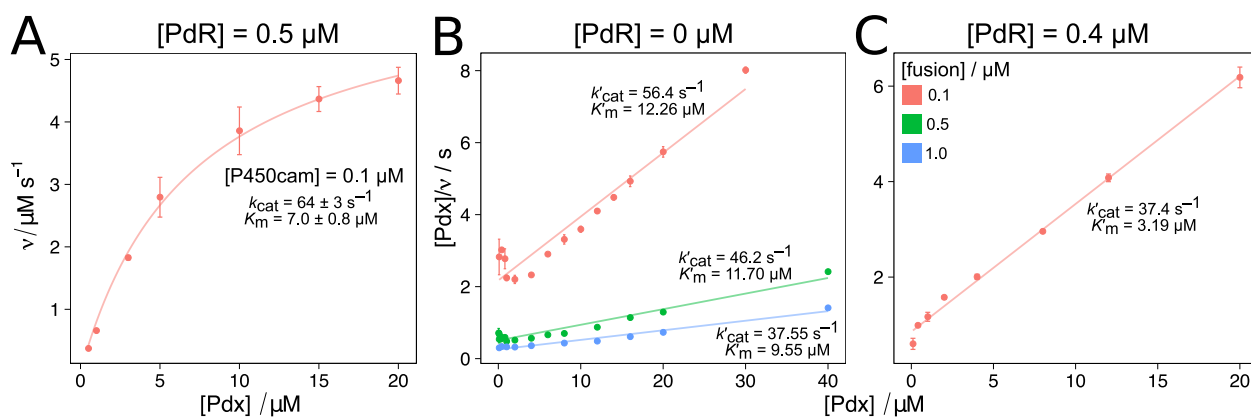
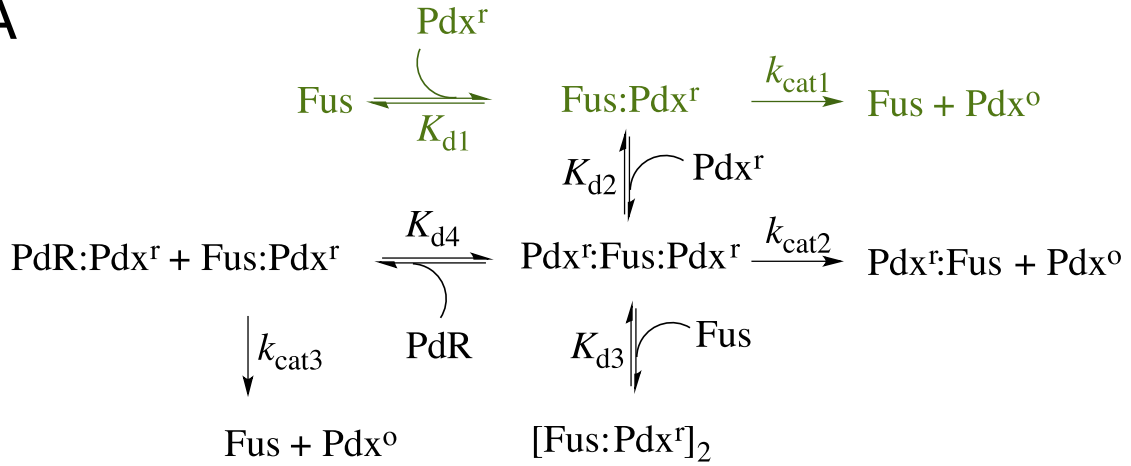


**Fig. 6. NADH oxidation kinetics of the reconstituted P450cam-L2-PdR fusion.** NADH oxidation by fused P450cam-PdR in the presence of Pdx was measured and compared to the native system. (A) The native P450cam system shows Michaelis-Menten kinetics. (B) Hanes-Woolf plots showing the non-Michaelis-Menten behavior of the P450cam-L2-PdR fusion: low Pdx concentrations give a deviation from linearity, and best-fit  $k_{\text{cat}}$ ,  $k'_{\text{cat}}$ , decreases as fusion concentration increases. Doping the system with PdR has similar but less pronounced behavior. (C) An equimolar amount of PdR was added to  $0.5 \mu\text{M}$  P450cam-PdR and Pdx was titrated across a similar concentration range. The kinetic behavior was different, with lower  $K_{\text{m}}$  and  $k_{\text{cat}}$  values.

A



B

$$-\frac{d[\text{NADH}]}{dt} = v = [\text{Fus}] \cdot \frac{k_{\text{cat}1} \frac{[\text{Pdx}]}{K_{d1}} + k_{\text{cat}2} \frac{[\text{Pdx}]^2}{K_{d1}K_{d2}} + k_{\text{cat}3} \frac{[\text{Pdx}]^2[\text{Fus}]}{K_{d1}K_{d2}K_{d3}}}{1 + \frac{[\text{Pdx}]}{K_{d1}} + \frac{[\text{Pdx}]^2}{K_{d1}K_{d2}} + \frac{[\text{Pdx}]^2[\text{Fus}]}{K_{d1}K_{d2}K_{d3}} + \frac{[\text{Pdx}]^2[\text{PdR}]}{K_{d1}K_{d2}K_{d4}}}$$

**Fig. 7. A proposed model for NADH oxidation kinetics of the reconstituted P450cam-L2-PdR fusion.** (A) Pdx<sup>r</sup>-to-P450cam electron transfer is the rate-limiting step of NADH oxidation. The native system conforms to the Michaelis-Menten model (green pathway). However, the P450cam-L2-PdR fusion deviates strongly from Michaelis-Menten behavior. An extended two-site sequential-binding model (green and black pathways) was proposed to explain the observed kinetics of the fused system. (B) Based on the proposed kinetic model, a function describing the initial rate of NADH oxidation in terms of enzyme concentrations could be derived, assuming instantaneous equilibrium.

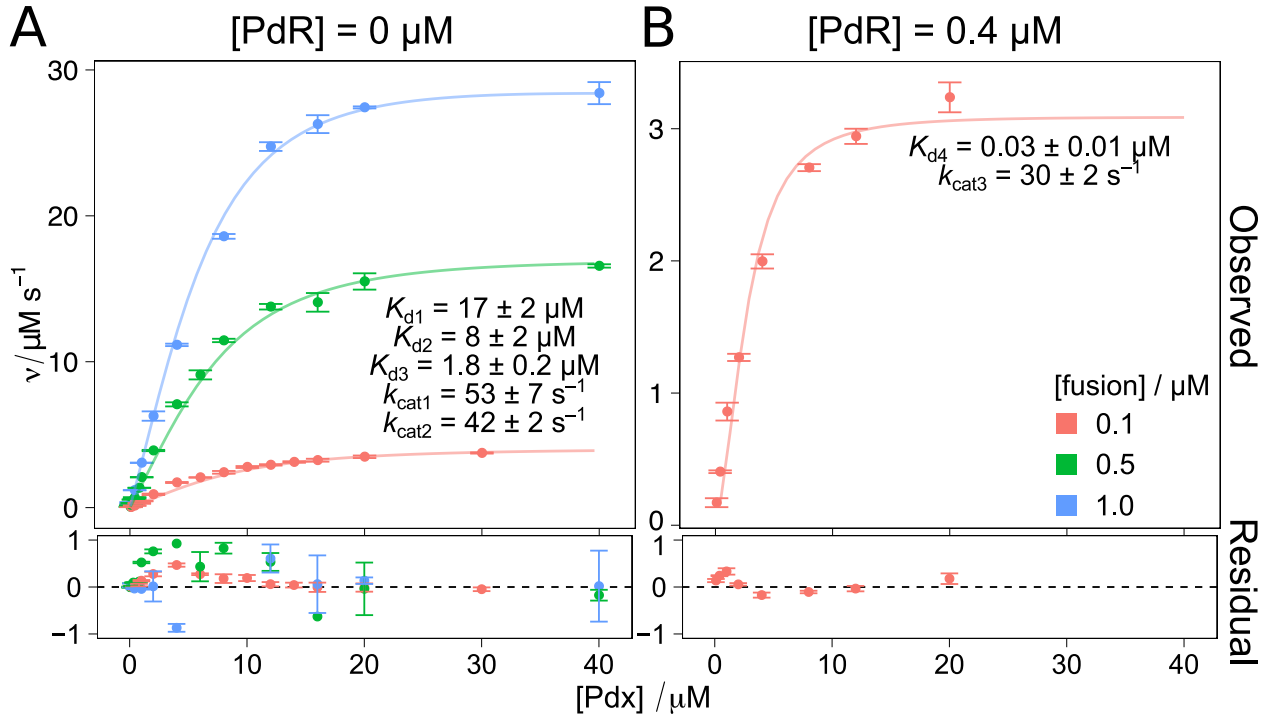


**Fig. 8. Best fit of the proposed kinetic model to the observed data.** (A–B) The model appears to explain the decrease in observed  $k_{cat}$  with increasing fusion concentration, along with apparent cooperativity at low Pdx concentrations. In addition, it explains the fused-native hybrid kinetics seen when the fusion was assayed in the presence of free PdR.